Multichromophoric Polymers

Investigation of Perylene Photonic Wires by Combined Single-Molecule Fluorescence and Atomic Force Microscopy**

Jordi Hernando, Pieter A. J. de Witte, Erik M. H.P van Dijk, Jeroen Korterik, Roeland J. M. Nolte, Alan E. Rowan, María F. García-Parajó, and Niek F. van Hulst*

Multichromophoric systems can exhibit interesting optical and electronic properties due to excitonic interactions between dye units that are near to each other.[1] An exquisite example found in nature is the light-harvesting antenna system in photosynthetic bacteria, which allow for efficient light absorption and unidirectional transfer of energy to the reaction center during photosynthesis.[2] The design of artificial multichromophoric arrays that mimic these properties is a great challenge, the ultimate goal being the construction of molecular photonic and electronic devices.

A unique insight into the physical behavior of multichromophoric systems is obtained with the help of single-molecule-detection techniques. Single-molecule force microscopy not only provides information on the dimensions of the aggregates but also on the internal organization of the chromophores,[1a,3] a crucial issue that governs their excitonic behavior. Single-molecule optical spectroscopy reveals characteristic features arising from exciton coupling, such as single-emitter behavior and collective fluorescent/nonfluorescent states, properties that otherwise remain hidden when probing the average behavior of ensembles of molecules.[4–6] In this work we have combined force and optical microscopy to investigate at the single-molecule level the properties of a new class of rigid multichromophoric polymers intended to act as synthetic antennas.

To attain optimal excitonic behavior in multichromophoric assemblies, a well-defined close packing of the chromophores is required. Recently, we have used intrinsically rigid and helical polymers of isocyanopeptides,[7] which have a persistence length of 76 nm,[8] as scaffolds to anchor porphyrin molecules. In this way long well-ordered porphyrin arrays with an average length of 87 nm were obtained.[9] In the work presented herein, we have used a similar approach to prepare perylene isocyano amino acid polymers. Perylene was chosen because of its: 1) high absorptivity and fluorescence quantum yield; 2) high thermal and high photochemical stability; 3) high electron affinity. Perylene-based chromophoric arrays[10] are promising components for the construction of optical and electronic molecular devices, for instance as n-type semiconductor material in organic photovoltaic cells.[11]

Figure 1 shows the structure of the perylene polyisocyanide **2**, as well as of the precursor perylene monomer **1**. A detailed description of the synthesis and characterization of **2**

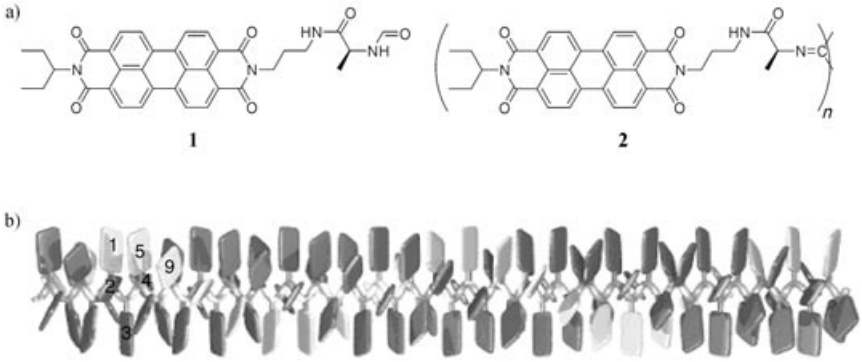

Figure 1. a) Structures of the perylene monomer (**1**) and the perylene polyisocyanide polymer (**2**); b) schematic 3D drawing of a molecule of polymer **2**. One perylene column is shown in light grey for clarity. Perylene units 1,5,9, and so on, belong to the same column.

will be given elsewhere.[12] Briefly, a monoamino perylene was coupled to Boc-L-alanine by using standard peptide coupling reagents. The resulting perylene-L-alanine product was formylated to yield product **1**, whose terminal *N*-formyl group was subsequently converted into an isocyanide. Polymerization of the latter species yielded perylene polyisocyanide **2**. Fractionation by the successive precipitation of redissolved polymer samples was used to purify perylene polyisocyanides from nonreacted monomers in the reaction mixture. This process was repeated until no changes in the bulk absorption and emission spectra of **2** were observed. The rodlike nature of the purified polymer **2** (see below) prevented us from obtaining information about its molecular weight and polydispersity by means of the usual techniques, such as MALDI-TOF, MS, or GPC.

The circular dichroism spectrum of **2** in $CHCl_3$ shows Cotton effects in the absorption region of perylene, as well as for the imine groups of the polyisocyanide backbone.[12] The latter Cotton effect is observed for polyisocyanides with

[*] Dr. J. Hernando, Ir. E. M. H. van Dijk, Ing. J. Korterik, Dr. M. F. García-Parajó, Prof. Dr. N. F. van Hulst
Applied Optics group
Faculty of Science and Technology
University of Twente and MESA+ Research Institute
P.O. Box 217, 7500AE Enschede (The Netherlands)
Fax: (+31) 53-489-3511
E-mail: m.f.garciaparajo@tnw.utwente.nl
P. A. J. de Witte, Prof. Dr. R. J. M. Nolte, Dr. A. E. Rowan
Department of Organic Chemistry, NSRIM
University of Nijmegen
Toernooiveld 1, 6525ED Nijmegen (The Netherlands)
Fax: (+31) 24-365-2929

[**] The authors thank E. E. Neuteboom, S. C. J. Meskers and R. A. J. Janssen for providing with the monomer precursor for the perylene polymer synthesis and their help with the ensemble fluorescence lifetime measurements. Financial support from the EC SMARTON network is gratefully acknowledged. J.H. thanks the EC Program IHP-99 for a Marie Curie Fellowship (HPMF-CT-2002-01698). E.M.H.P.v.D. thanks the support by Dutch Foundation for Fundamental Research of Matter (FOM). M.F.G.P. acknowledges support from KNAW.

 DOI: 10.1002/anie.200453745

alanine dipeptide sidegroups that form hydrogen-bonding arrays along the polymer.[13] This provides us with a clear signature indicating that polymer **2** has a rigid helical backbone, which is stabilized through a hydrogen-bonding network between the amino acid side chains, as shown schematically in Figure 1b. The perylene chromophores are attached to this backbone in four parallel stacks. For the previously synthesized porphyrin polyisocyanides,[9] the adjacent dye molecules in one stack were found to be 4.2 Å apart with a twist angle of 22°. Similar values are expected for the perylene polyisocyanide **2**. For such a chromophoric close-packing, an optical behavior governed by excitonic interactions is anticipated. This is demonstrated by the bulk absorption and fluorescence emission spectra of **1** and **2** in $CHCl_3$ (Figure 2). Compared to the monomer, the peak

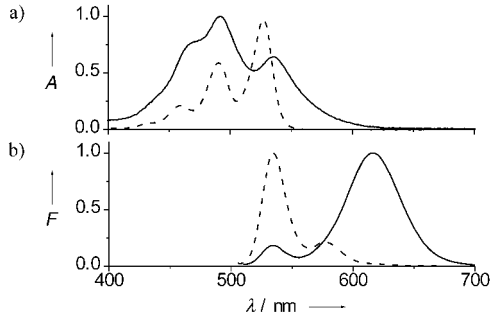

Figure 2. a) Absorption (*A*, arbitrary units) and b) fluorescence (*F*, arbitrary units) emission spectra of monomer **1** (dashed line) and polymer **2** (continuous line) in $CHCl_3$.

positions in the absorption spectrum of the polymer and their relative intensities have changed. These differences indicate that interaction between the perylene units in **2** already occurs in the ground state, pointing to the existence of excitonic effects. According to exciton theory[14] we assign the blue-shifted peak at $\lambda = 492$ nm to the interaction, parallel to the axis of the system, between the nearly face-to-face 1st, 5th, 9th, etc. perylene units, while the slightly red-shifted band at $\lambda = 536$ nm is ascribed to coupling between the 1st, 2nd, 3rd, and 4th dyes in the plane perpendicular to the axis of the polymer. The overlay of these two exciton bands and their vibronic peaks explains the broadening and apparent loss of structure of the polymer absorption spectrum. The fluorescence properties of the polymer are even more distinct: a broad structureless red-shifted band is visible, the quantum yield has decreased ($\Phi = 0.11$) and the fluorescence decay is multiexponential, with a minor contribution from a decay time equal to that of **1** ($\tau_1 = 3.9$ ns) and a major contribution from a much longer decay time ($\tau_2 = 19.9$ ns).[12] These features demonstrate that emission mainly arises from intramolecular excimer-like species in the polymer, a phenomenon known to occur in stacks of perylene molecules.[6,15] Although interaction in the ground state may also contribute to the formation of excimer-like species in the polymer,[16] this process essentially occurs upon irradiation of proximal chromophores, whose conjugation paths fully or partially overlap, as perylene units 1, 5, 9, etc. do in polymer **2**.

Diluted solutions of **2** in $CHCl_3$ were investigated by atomic force microscopy (AFM) after spin-coating on mica. Isolated single perylene polyisocyanide polymer molecules of different lengths were observed in the AFM images as shown in Figure 3. Fibers up to a few hundreds of nanometers in

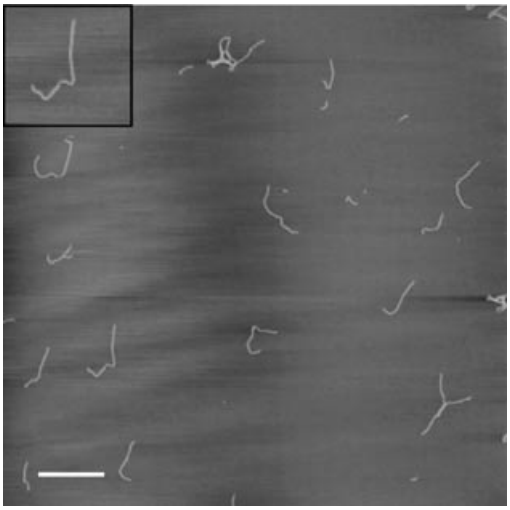

Figure 3. AFM image of a diluted solution of polymer **2** spin-coated on mica. Inset: enlargement of an individual fiber (bar = 500 nm).

length and about 2.5 nm in height are present, consistent with single helical perylene polyisocyanide polymer fibers being probed. In the absence of well-defined helical structure the height of the polymers should be much lower and thus not resolvable with AFM.

Detailed insight into the photophysical properties of individual perylene polyisocyanides was obtained by performing single-molecule fluorescence imaging of diluted solution of **2** in $CHCl_3$ after spin-coating on glass. Subsequently, the evolution of the emission intensity and fluorescence spectra of individual polymer fibers was recorded as a function of time. Two different species with distinct emissive behaviors were distinguished in the polymer sample. In the following discussion, we refer to these two types of molecules as green and red species owing to their different fluorescence spectra. The intensity time trajectories for two typical green and red species are shown in Figure 4 together with their fluorescence spectra integrated over the whole $t = 0$–25 s time window. A decrease in the fluorescence intensity with time was observed for both species, a process known to occur for multichromophoric systems due to successive photodegradation of the multiple emitting sites in the aggregate.[4–6] However, whereas a continuous decrease in fluorescence was measured for the red species, distinct and discrete intensity levels occurred for the green-fluorescent spot. These observations indicate that the latter species consisted of a few emitting units, while the former species contained a large number of independent fluorescent sites, as observed in conjugated polymers.[5b] The occurrence of a collective nonfluorescent state ($t = 3.5$–7.5 s) for the highest intensity level of the green species may arise from the photodriven generation of a long-lived trapped species fully quenching the fluorescence of the system, a

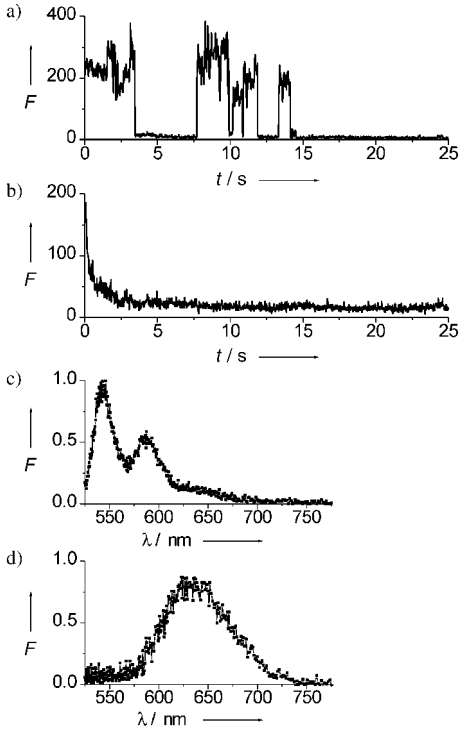

Figure 4. Fluorescence intensity trajectory for green (a) and red (b) single molecules; their emission spectra integrated over the whole $t = 0$–25 s time window are given in plots c) and d), respectively.

behavior usually ascribed to radical formation in perylene aggregates.[6,17] Spectral measurements were found to cast some light on the nature of these two types of fluorescent compounds. For the green species, the fluorescence spectrum resembled that of monomer **1**, which display the characteristic vibronic peaks for perylene emission. The red species, however, showed a broader red-shifted fluorescence spectrum indicating that the emission mainly arose from excimer-like sites, as observed for polymer **2** in solution. No significant spectral changes were observed during the emission period of both molecules.

The spread in fiber lengths as shown in Figure 3 suggests that the two emissive behaviors may arise from heterogeneity in the polymer structure. To investigate such a situation, simultaneous topographical and optical measurements on individual perylene polyisocyanides were performed. Figure 5 shows AFM and fluorescence images recorded on the same area of a spin-coated sample **2** on glass. Single polymer fibers with helical backbones (height ≈ 2.5 nm) are observed in the AFM picture; the length of these fibers vary between 20 to 120 nm. The emission arising from single fluorescent species is displayed in the fluorescence image. Green and red spots correspond to species emitting at $\lambda < 590$ nm and $\lambda > 590$ nm, respectively, which allowed us to distinguish between green ($\lambda < 590$ nm) and red species ($\lambda > 590$ nm). Clearly, a correlation between topography and fluorescence signal is only observed for those molecules emitting in the red, while green-fluorescent species do not show any counterpart feature in the AFM image.

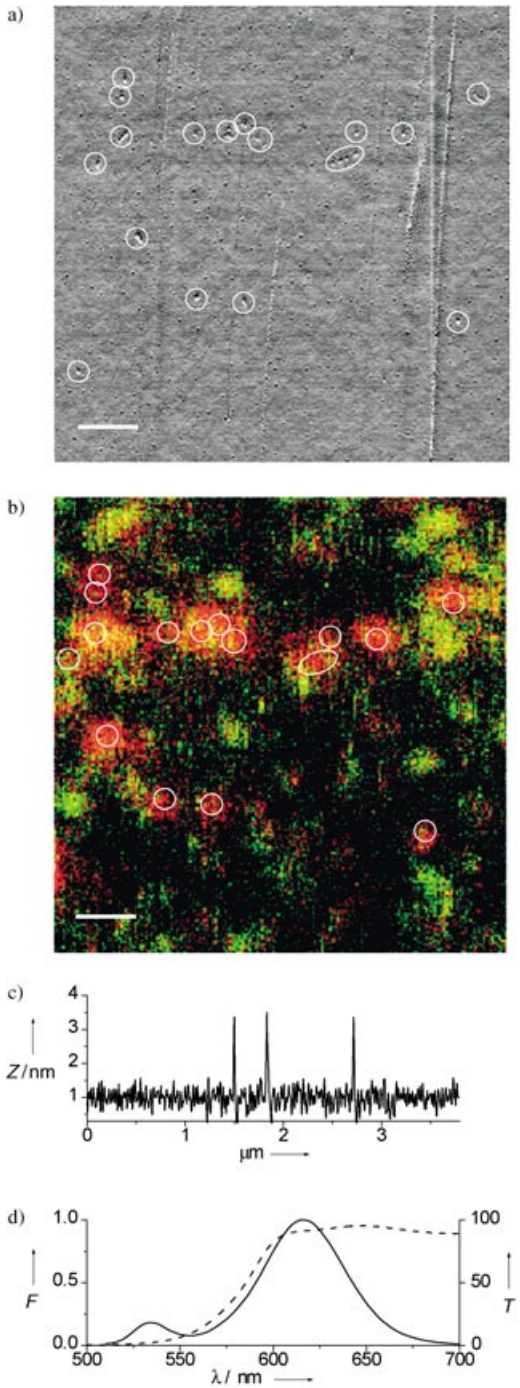

Figure 5. a) AFM and b) confocal fluorescence images from the same $3.8 \times 3.8\ \mu m^2$ area of a diluted solution of polymer **2** spin-coated on glass (bar = 500 nm); c) height profile (Z) for a line section of the AFM image; d) bulk fluorescence emission spectrum of polymer **2** in $CHCl_3$ (continuous line) and transmitance spectrum of the dichroic beam splitter used to distinguish between green ($\lambda < 590$ nm) and red ($\lambda > 590$ nm) fluorescent molecules (dashed line).

As the red emission originates from the single polymer fibers visualized in the topography image, we conclude that the helical perylene polyisocyanides emit through multiple independent excimer-like sites created along the fiber. After excitation of the polymer, we expect strong coupling between

proximal perylene units, thus allowing exciton delocalization.[18] However, this process would be rapidly quenched by the formation of excimer-like species caused by the interaction between two or a few nearly cofacial perylenes. These perylenes act as a sink for the exciton, thus limiting the extent of the delocalization of the electronic excitation, and ultimately they are responsible for the polymer emission. Exploiting our combined single-molecule topography and fluorescence technique, we investigated the correlation between polymer length and emission intensity. The results obtained are presented in Figure 6, which shows the dependence of the fluorescence intensity (at $t=0$) arising from helical perylene polysisocyanides as a function of the polymer length. A clear linear correlation between these two parameters is found, which indicates that the longer the polymer, the higher the absorption and the number of excimer-like sites susceptible to be formed and, therefore, the stronger the polymer emission. Furthermore, the linear trend found in Figure 6 demonstrates that there are no saturation effects at the power density used to excite the molecules.

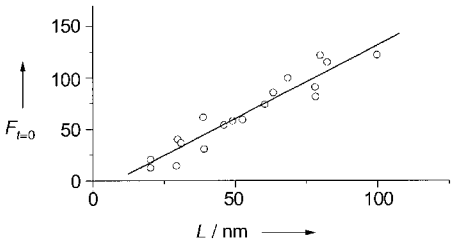

Figure 6. Plot of the fluorescence intensity (taken at $t=0$) versus the polymer length (L) for 18 single perylene polyisocyanide molecules. The values plotted in the length axis do not correspond to the actual length of the polymers but to the convolution between their length and the tip size, which explains why the line fit does not go through the origin.

On the other hand, we assign the green emission to short polyisocyanides oligomers consisting of only a few perylene units.[19] For these species, no helical structure of the polymer backbone is expected.[20] Accordingly, their height is much lower than the height of the helical polyisocyanides and therefore below the sensitivity of our AFM head (≈ 1 nm[21]), thus explaining why no correlated topography signal is obtained.[22] As there is an absence of a helical conformation, the interchromophoric distances between adjacent perylene units in polymer **2** will be much longer; consequently weaker (if any) excitonic effects without formation of excimer-like species are expected. This accounts for the fact that their fluorescence spectrum is the same as that of monomer **1**. The quantum yield of fluorescence for the short perylene oligomers undergoing weak excitonic interactions is expected to be similar to that of the monomer; however, the quantum yield of perylene excimer-like species is known to be much lower.[15] This partially explains why the overall fluorescence count rate arising from helical perylene polyisocyanides that contains hundreds to thousands chromophore units is in the same order of magnitude as that for the few-perylene nonhelical oligomers, as observed for the green and red species in Figure 4. In addition, the low fluorescence yield of the long helical polymers may also be due to charge separation and intramolecular electron transfer upon optical excitation, as recently suggested for perylene dimers with short interchromophoric distances.[17]

In summary, we have combined single-molecule confocal fluorescence and atomic force microscopy to unambiguously characterize a new class of multichromophoric polymers, namely perylene polyisocyanides. Our single-molecule measurements show that the synthesized perylene arrays are heterogeneous in nature, which we ascribe to distinct structures of the polymer backbone. Thus, short nonhelical perylene oligomers display monomer-like fluorescence properties, whereas long helical perylene polymer emission arises from multiple and independent excimer-like sites. Although the formation of the latter species prevents delocalization of the excitation energy along the polymer backbone over large distances, its long fluorescence decay time may favor the use of the polymers as n-type semiconductor in bulk-heterojunction solar cells.

Experimental Section

Atomic force microscopy**:** AFM experiments were performed by using a Nanoscope IIIa instrument from Digital Instruments. All images were recorded in tapping mode in air at room temperature.

Combined confocal fluorescence and atomic force microscopy: Fluorescence from single molecules was detected by means of a confocal scanning fluorescence microscope, as described elsewhere.[5c] Circularly polarized excitation light at $\lambda = 488$ nm with a power density at the sample 1–2 kW cm^{-2} was used. The fluorescence signal was detected by two avalanche photodiodes (APD, SPCM-AQ-14, EG&G Electro Optics) and a CCD camera (Andor, DV437-BV). A dichroic beam splitter (Omega, 590DRLP) in front of the APDs splitted the fluorescence into two distinct spectral windows (APD1: $\lambda < 590$ nm; APD2: $\lambda > 590$ nm; see Figure 5). A direct vision prism in front of the CCD camera spread the emission light over its wavelength components. Fluorescence spectra were collected by using an integration time of 1 s. A home-made AFM head[23] was placed on top of the confocal microscope to perform combined topography and fluorescence measurements for single molecules. All images were recorded in tapping mode in air at room temperature.

Received: January 13, 2004
Revised: April 30, 2004 [Z53745]

Keywords: fluorescence spectroscopy · nanotechnology · photochromism · scanning probe microscopy · single-molecule studies

[1] a) D. A. Higgins, J. Kerimo, D. A. Vanden Bout, P. F. Barbara, *J. Am. Chem. Soc.* **1996**, *118*, 4049–4058; b) V. Balzani, F. Scandola in *Comprehensive Supramolecular Chemistry: Supramolecular Technology, Vol. 10* (Eds.: J. L. Atwood, J. E. D. Davies, D. D. Macnicol, F. Vögtle, D. N. Reinhoudt), Pergamon, Oxford, **1996**, p. 687.

[2] T. Pullerits, V. Sundström, *Acc. Chem. Res.* **1996**, *29*, 381–389; X. Hu, A. Damjanović, T. Ritz, K. Schulten, *Proc. Natl. Acad. Sci. USA* **1998**, *95*, 5935–5941.

[3] S. Scheuring, F. Reiss-Husson, A. Engel, J. L. Rigaud, J. L. Ranck, *EMBO J.* **2001**, *20*, 3029–3035; A. Stamouli, S. Kafi, D. C. G. Klein, T. H. Oosterkamp, J. W. M. Frenken, R. J. Cogdell, T. J. Aartsma, *Biophys. J.* **2003**, *84*, 2483–2491.

[4] M. Wu, P. M. Goodwin, W. P. Ambrose, R. A. Keller, *J. Phys. Chem.* **1996**, *100*, 17406 – 17409; M. A. Bopp, Y. W. Jia, L. Q. Li, R. J. Cogdell, R. M. Hochstrasser, *Proc. Natl. Acad. Sci. USA* **1997**, *94*, 10630 – 10635; L. Ying, X. S. Xie, *J. Phys. Chem. B* **1998**, *102*, 10399 – 10409; M. F. García-Parajó, M. Koopman, E. M. H. P. van Dijk, V. Subramaniam, N. F. van Hulst, *Proc. Natl. Acad. Sci. USA* **2001**, *98*, 14392 – 14397, and references therein.

[5] a) D. A. Vanden Bout, W.-T. Yip, D. Hu, D.-K. Fu, T. M. Swager, P. F. Barbara, *Science* **1997**, *277*, 1074 – 1077; D. Hu, J. Yu, P. F. Barbara, *J. Am. Chem. Soc.* **1999**, *121*, 6936 – 6937; J. Hofkens, W. Schroeyers, D. Loos, M. Cotlet, F. Köhn, T. Vosch, M. Maus, A. Herrmann, K. Müllen, T. Gensch, F. C. De Schryver, *Spectrochim. Acta Part A* **2001**, *57*, 2093 – 2107; C. Hettich, C. Schmitt, J. Zitzmann, S. Kühn, I. Gerhardt, V. Sandoghdar, *Science* **2002**, *298*, 385 – 389; P. Tinnefeld, K. D. Weston, T. Vosch, M. Cotlet, T. Weil, J. Hofkens, K. Mullen, F. C. De Schryver, M. Sauer, *J. Am. Chem. Soc.* **2002**, *124*, 14310 – 14311; C. G. Hubner, G. Zumofen, A. Renn, A. Herrmann, K. Mullen, T. Basché, *Phys. Rev. Lett.* **2003**, *91*, 093903; T. Vosch, M. Cotlet, J. Hofkens, K. Van Der Biest, M. Lor, K. Weston, P. Tinnefeld, M. Sauer, L. Latterini, K. Mullen, F. C. De Schryver, *J. Phys. Chem. A* **2003**, *107*, 6920 – 6931; b) T. Huser, M. Yan, L. J. Rothberg, *Proc. Natl. Acad. Sci. USA* **2000**, *97*, 11187 – 11191; c) J. Hernando, M. van der Schaaf, E. M. H. P. van Dijk, M. Sauer, M. F. García-Parajó, N. F. van Hulst, *J. Phys. Chem. A* **2003**, *107*, 43 – 52.

[6] J. Hofkens, M. Maus, T. Gensch, T. Vosch, M. Cotlet, F. Köhn, A. Herrmann, K. Müllen, F. C. De Schryver, *J. Am. Chem. Soc.* **2000**, *122*, 9278 – 9288; T. Vosch, J. Hofkens, M. Cotlet, F. Köhn, H. Fujiwara, R. Groenheid, K. van der Biest, T. Weil, A. Herrmann, K. Müllen, S. Mukamel, M. van der Auweraer, F. C. De Schryver, *Angew. Chem.* **2001**, *113*, 4779 – 4784; *Angew. Chem. Int. Ed.* **2001**, *40*, 4643 – 4648.

[7] J. J. L. M. Cornelissen, J. J. J. M. Donners, R. de Gelder, W. S. Graswinckel, G. A. Metselaar, A. E. Rowan, N. A. J. M. Sommerdijk, R. J. M. Nolte, *Science* **2001**, *293*, 676 – 680.

[8] P. Samori, C. Ecker, I. Gossl, P. A. J. de Witte, J. J. L. M. Cornelissen, G. A. Metselaar, M. B. J. Otten, A. E. Rowan, R. J. M. Nolte, J. P. Rabe, *Macromolecules* **2002**, *35*, 5290 – 5294.

[9] P. A. J. de Witte, M. Castriciano, J. J. L. M. Cornelissen, L. Monsû-Scolaro, R. J. M. Nolte, A. E. Rowan, *Chem. Eur. J.* **2003**, *9*, 1775 – 1781.

[10] H. Langhals, W. Jona, *Angew. Chem.* **1998**, *110*, 998 – 1001; *Angew. Chem. Int. Ed.* **1998**, *37*, 952 – 955; L. H. Gade, C. H. R. M. Williams, L. De Cola, M. McPartlin, B. Dong, L. Chi, *Angew. Chem.* **2003**, *115*, 2781 – 2785; *Angew. Chem. Int. Ed.* **2003**, *42*, 2677 – 2681.

[11] N. Noma, T. Tsuzuki, Y. Shirota, *Adv. Mater.* **1995**, *7*, 647 – 648; T. Toshimitsu, N. Hirota, N. Noma, *Thin Solid Films* **1996**, *273*, 177 – 180.

[12] P. A. J.de Witte, J. Hernando, E. E. Neuteboom, S. C. J. Meskers, R. A. J. Janssen, M. F. García-Parajó, N. F. van Hulst, R. J. M. Nolte, A. E. Rowan, *J. Am. Chem. Soc.*, submitted.

[13] J. J. L. M. Cornelissen, W. S. Graswinckel, P. J. H. M. Adams, G. H. Nachtegaal, A. P. M. Kentgens, N. A. J. M. Sommerdijk, R. J. M. Nolte, *J. Polym. Sci. Part A* **2001**, *39*, 4255 – 4264.

[14] M. Kasha, H. R. Rawls, M. Ashaf El-Bayoumi, *Pure Appl. Chem.* **1965**, *37*, 371; M. Bednarz, J. Knoester, *J. Phys. Chem. B* **2001**, *105*, 12913 – 12923.

[15] W. E. Ford, P. V. Kamat, *J. Phys. Chem.* **1987**, *91*, 6373 – 6380; P. B. Bisht, K. Fukuda, S. Hirayama, *Chem. Phys. Lett.* **1996**, *258*, 71 – 79; S. Akimoto, A. Ohmori, I. Yamazaki, *J. Phys. Chem. B* **1997**, *101*, 3753 – 3758, and references therein.

[16] P. Reynders, W. Kuhnle, K. A. Zachariasse, *J. Phys. Chem.* **1990**, *94*, 4073 – 4082.

[17] R. Liu, M. W. Holman, L. Zang, D. M. Adams, *J. Phys. Chem. B* **2003**, *107*, 6522 – 6526.

[18] For the related porphyrin polymer, excitonic interaction extends over domains larger than 25 dye units (see reference [9]).

[19] The same sort of behavior will be observed for the unconverted monomer molecules left in the purified polymer sample as well.

[20] Studies on polyisocyanides have proven that at least 10–15 repeat units are necessary for the helical structure to be stable.

[21] This is the average noise level in our AFM images (see Figure 4c). Two main factors are limiting our sensitivity: 1) the roughness of the substrate (O_2 plasma cleaned cover glass, which shows much better optical properties than mica) and 2) the vibrations induced by the immersion oil underneath the coverglass.

[22] Repetitive fluorescence scans on the same area before and after AFM detection allows us to rule out the possibility of spontaneous and tip-induced movement of the green species as the origin for their nonobservance in the topography image.

[23] K. O. van der Werf, C. A. Putman, B. G. de Grooth, F. B. Segerink, E. H. Schipper, N. F. van Hulst, J. Greve, *Rev. Sci. Instrum.* **1993**, *64*, 2892 – 2897.

